Article

Not peer-reviewed version

# Method and Experiment for Quantifying Local Features of Hard Bottom Contours of Intelligent Farm Machinery Driving in Paddy Fields

Tuanpeng Tu , Lian Hu , Xiwen Luo , Jie He * , Pei Wang , Li Tian , Gaolong Chen , Zhongxian Man , Dawen Feng , Weirui Cen , Mingjin Li , Yuxuan Liu , Kang Hou , Le Zi , Mengdong Yue , Yuqin Li

Posted Date: 4 July 2023

doi: 10.20944/preprints202307.0027.v1

Keywords: Hard bottom layer; Surface profile features; Local roughness; Unmanned farms; Smart farming machines

*Article*

# Method and Experiment for Quantifying Local Features of Hard Bottom Contours of Intelligent Farm Machinery Driving in Paddy Fields

**Tuanpeng Tu [1,2], Lian Hu [1,2], Xiwen Luo [1,2], Jie He [1,2,*], Pei Wang [1,2], Li Tian [1,2], Gaolong Chen [1,2], Zhongxian Man [1,2], Dawen Feng [1,2], Weirui Cen [1,2], Mingjin Li [1,2], Yuxuan Liu [1,2], Kang Hou [1,2], Le Zi [1,2], Mengdong Yue [1,2] and Yuqin Li [1,2]**

[1] Key Laboratory of the Ministry of Education of China for Key Technologies for Agricultural Machinery and Equipment for Southern China, South China Agricultural University, Guangzhou 510642, China; 1024462631@qq.com (T.T.) ; lianhu@scau.edu.cn (L.H.); xwluo@scau.edu.cn (X.L.); hooget@scau.edu.cn(J.H.); peiwang@scau.edu.cn (P.W.); 1479945492@qq.com (L.T.); dbalong@163.com (G.C.); 371270285@qq.com (Z.M.); fdw_199701@163.com (D.F.); 532089300@qq.com (W.C.); 244700076@qq.com (M.L.); 1031067913@qq.com (Y.L.); 1921169638@qq.com (K.H.); 2315987276@qq.com (L.Z.); 760584484@qq.com (M.Y.); 2568378686@qq.com (Y.L.)

[2] Guangdong Laboratory for Lingnan Modern Agriculture , Guangzhou 510642, China; 1024462631@qq.com (T.T.) ; lianhu@scau.edu.cn (L.H.); xwluo@scau.edu.cn (X.L.); hooget@scau.edu.cn(J.H.); peiwang@scau.edu.cn (P.W.); 1479945492@qq.com (L.T.); dbalong@163.com (G.C.); 371270285@qq.com (Z.M.); fdw_199701@163.com (D.F.); 532089300@qq.com (W.C.); 244700076@qq.com (M.L.); 1031067913@qq.com (Y.L.); 1921169638@qq.com (K.H.); 2315987276@qq.com (L.Z.); 760584484@qq.com (M.Y.); 2568378686@qq.com (Y.L.)

* Correspondence: hooget@scau.edu.cn; Tel.: +86-13922135357

**Abstract:** The hard bottom layer of paddy field has a great influence on the driving stability and operation quality and efficiency of intelligent farm machinery, and the continuous improvement of unmanned precision operation accuracy and operation efficiency of paddy field operation machin-ery is the support to realize unmanned rice farm. In this paper, in view of the complicated hard bottom layer situation of unmanned operation farm machinery driving is difficult to realize to quantify the local characteristics of hard bottom layer of paddy field, the unmanned rice direct seeding machine chassis is used to operate the operation field and collect the hard bottom layer information simultaneously, and the data processing method of automatic calibration of sensor installation error, abnormal value rejection and 3D sample curve denoising of contour trajectory is designed; a hard bottom layer surface profile evaluation method based on the local sliding surface roughness is proposed. The local characteristics of the hard bottom layer were quantified, and the quantified results of the local characteristics of the hard bottom layer in the test plots showed that the mean value of the local roughness was 0.0065, 68.27% was distributed in the variation range of 0.0042~0.0087, and 99.73% was distributed in the variation range of 0~0.0133. Based on the test field data, the surface roughness features are verified to describe the variability of representative working conditions such as transport, downfield, operation and trapping of unmanned operation of intelligent farm machinery. The method of quantifying the hard-bottom local features of farm machinery driving can provide feedback on the local environmental features of intelligent farm machinery driving at the current position, and provide a reference basis for the design optimization of unmanned system for improving the quality of intelligent farm machinery operation.

**Keywords:** hard bottom layer; surface profile features; local roughness; unmanned farms; smart farming machines

## 1. Introduction

Rice, as a major food source for more than 50% of the global population [1] , is an important supporting food crop for the United Nations to achieve the Sustainable De-velopment Goal (SDG) of

zero hunger by 2030 [2] .China ranks second in the world in terms of rice cultivation area, with 29.4 million ha under perennial cultivation, accounting for about 19% of the world and nearly 30% of the global rice production [3]. From 2010 to 2016, the net increase in the area of paddy and watered land in China was 356,000 ha [4], showing a net increasing trend. Agricultural machinery intelligence and information technology is an inevitable trend of modern agricultural production and an effective way to develop efficient and costsaving agriculture [5,6], and it is important to accelerate the development of agriculture from mechanization to intelligence and improve the level of agricultural equipment intelligence [7]. It is very important to promote the transformation and upgrading of agricultural equipment and agricultural mechanization, and to enhance the modernization of largescale operations of rice and other crops. More and more unmanned intelligent farm equipment for rice production will be put into paddy fields for application to meet the needs of precise rice production [8].

The hard bottom layer of paddy field has a great influence on the driving stability and operation quality and efficiency of intelligent farm machinery. The unmanned farm machine travels on the hard bottom layer of the paddy field contour features potholes and ditches of varying depths, which causes the vibration of farm machinery and interferes with the steady state motion in the longitudinal, lateral and transverse pendulum directions, making the unmanned farm machine prone to sudden changes in motion such as side slip, leading to its operation at the set speed with significantly reduced and inconsistent control accuracy, which seriously affects the operation quality and efficiency, resulting in the unmanned highspeed operation failing to achieve the expected results [9], which to a certain extent restricts the application of unmanned farming machines in unmanned farms. To provide feedback of hard-bottom layer features of driving for unmanned farm machine control, to provide reference basis for unmanned farm machine operation control system, and to realize unmanned precise and high quality and efficient operation of paddy field operation machinery, it is urgent to obtain hard-bottom layer local features of unmanned farm machine driving and establish quantitative expression method.

In terms of acquiring farmland topography, laser technology [10] and GNSS tech-nology were combined with grader to achieve realtime acquisition of 3D topography of farmland mud surface after grading [11-14], respectively. Francisco Rovira-Mas et al. constructed a 3D scene terrain generation system using stereo camera, RTK GPS, and fiber optic gyroscope (FOG) for automatic field tractor navigation [15] ; Marinello et al. and Yandun Narvaez et al. used RGB depth camera obtained dynamic characteristics of soil morphology in agricultural fields [16,17]. Man Zhang et al. constructed a 3D terrain information measurement system using RTD-DGPS and laser measurement technology [18], which provides a solution for topographic measurement. Starek et al. used Kriging spatial interpolation method for wide area terrain prediction and modeling based on total station high density laser scanned point cloud [19]. Tuanpeng Tu et al. combined GNSS and AHRS technologies to achieve hard substrate contour acquisition and digital representation of paddy fields using an unmanned rice direct seeding machine chassis with elevation standard error less than 2 cm [20].

In terms of terrain feature measurement, research in the field of vehicle engineering and highway engineering has focused on the description and evaluation of unevenness, numerical modeling and simulation of road surface contours, and the effect of unevenness on automatic control and vehicle dynamics performance. Researchers have used a variety of sensing devices to measure road surface contours [21-23] and expressed the power spectral density of pavement displacement according to ISO/TC 108 (1972) and GB 7031-86 using a power function form to calculate the power spectral density ( Power spectral density (PSD), and a unified description and evaluation classification (A - H) of pavement unevenness was given based on the international standard ISO 8608: 2016. In the expression of farmland topographic features, Zhanfeng Hou et al. and Zhixiong Lu et al. used laser-type unevenness testers to determine the unevenness of plow plowed land, disc harrow harrowed land and driven harrow harrowed land, and proposed the concept of unevenness index, which proved that the pavement unevenness index has the uniqueness of describing pavement unevenness and is one of the main indicators for pavement grading [24,25]. Lijuan Wang et al. designed an agricultural ground unevenness testing device consisting of two trapezoidal bumps of

 doi:10.20944/preprints202307.0027.v1



known dimensions [26]. Sihong Zhu et al. used a level to measure the elevation change of a tire attached to an undulating hard subgrade of a paddy field under certain pressure [27], and Runmao Zhao et al. collected elevation unevenness information of a paddy field hard subgrade based on vehicle vibration response and GNSS elevation positioning information, indicating that the paddy field hard subgrade unevenness grade was between C and E [28].

The above research can realize the mapping of mud surface or hard substrate of roads and farmlands and grading their unevenness; using the parameters of road surface unevenness to measure and evaluate farmlands and realize the macro statistics of farmland leveling degree. However, for the local feature expression of different areas of the hard bottom layer of paddy fields, it is impossible to obtain the hard bottom layer feature parameters that affect the operational performance of unmanned farm machinery in a small area, and it is difficult to realize the local situation expression of the hard bottom layer of farm machinery driving, and there is a lack of a local feature quantification expression method for the hard bottom layer contour of paddy fields.

In this paper, for the hard bottom layer driven by unmanned operation of intelligent farming machine, it is difficult to meet the problem of local feature expression by expressing its features only with unevenness, adopting the unmanned rice direct seeding machine chassis to operate the operation field and collect the hard bottom layer information simultaneously, and designing the data processing method of automatic calibration of sensor installation error, outlier rejection and 3D sample curve denoising of contour trajectory. Adopt the method of calculating local sliding surface roughness to evaluate the degree of hard bottom surface roughness and quantify the local characteristics of hard bottom layer in paddy fields; analyze the representative driving route surface roughness characteristics of unmanned operation of intelligent farming machine including transportation, down-field, operation and trapping, and verify the difference based on the data of test field plots. Provide feedback on the local environmental characteristics of the current location driving for the intelligent farm machine, and provide reference basis for the design optimization of unmanned system for improving the quality of intelligent farm machine operation.

## 2. Materials and Methods

### *2.1. Hard-bottom contour sensing platform*

The hard-bottom contour sensing platform is selected to design a paddy field hard-bottom acquisition platform, which uses an unmanned rice direct seeding machine without damping suspension in the rear axle as a power chassis. GNSS and AHRS are installed on the frame, and the unmanned system is used to collect the vehicle position and attitude information simultaneously. The spatial position point set of the contact between the rear wheel bottom and the hard bottom layer of the agricultural machine was obtained by coordinate conversion of the vehicle body position information and vehicle body attitude information, which can realize the direct and continuous acquisition of the hard bottom layer contour information of the paddy field through the paddy field water layer and tillage layer, and the accuracy of the hard bottom layer contour measurement can reach 1.55 cm [20]. The paddy field hard substrate contour sensing platform is shown in Figure 1.

Preprints (www.preprints.org) | NOT PEER-REVIEWED | Posted: 4 July 2023 doi:10.20944/preprints202307.0027.v1



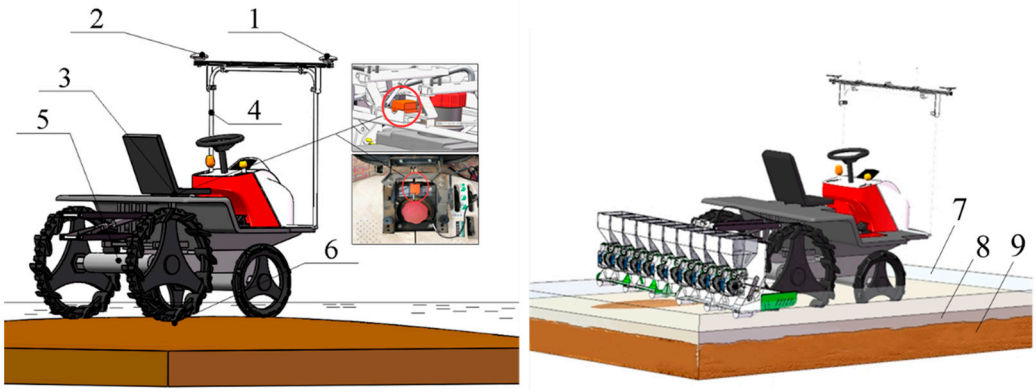


1. Primary positioning antenna 2. Slave-positioning antenna 3. AHRS 4. Support frame 5. Unmanned direct seeding machine chassis 6. Mapping point at the bottom of right rear wheel 7.Water layer 8. Tillage layer 9. Hard bottom later

**Figure 1.** Collection platform mounted on the chassis of the unmanned direct seeding machine.

*2.2. The method of processing the collected data*

2.2.1. Automatic calibration of sensor mounting errors

When sensors and their components are installed on different farm machinery chassis separately, it is difficult to ensure the relative positions of GNSS dual antenna and AHRS sensor installation positions are consistent because of mechanical structure size deviation, assembly deviation and installation deviation, so the initial positions of sensor installation need to be calibrated before intelligent farm machinery operation. In order to quickly obtain the system deviations generated by the installation of the attitude sensors and compensate them automatically, round-trip linear driving on the same path is used to analyze and calibrate the acquired heading angle, cross-roll angle and pitch angle data, and the implementation method is as follows:

(1) Automatic calibration of heading angle

When the farm machinery travels in a straight line, the heading value recorded by the dual antennas is recorded, and the point set of the main positioning antennas positioned in the straight line travel trajectory is obtained at the same time, and a straight line is fitted to the point set, and the direction of the fitted straight line is the real heading of the farm machinery, and the line model constructed by the fitting is shown in Equation (1).

$$y = kx + b \tag{1}$$

Where, $x$ is the coordinate value of the main antenna positioned due east, $y$ is the coordinate value of the main antenna positioned due north, $k$ is the slope of the fitted line, and $b$ is the intercept of the fitted line.

According to the single antenna heading linear fitting model, it is known that the true heading angle of the vehicle is the arctangent of the slope of the fitted straight line, as shown in Equation (2).

$$Yaw_d = \arctan(k \cdot \frac{180}{\pi}) \tag{2}$$

where, $Yaw_d$ is the single antenna heading angle.

The single antenna heading angle is compared with the average value of the recorded dual antenna heading angle, and the difference between the measured heading angle of the dual antenna and the real heading angle of the vehicle is obtained, that is, the installation error of the dual antenna is obtained, as shown in Equation (3).

$$E_{Yaw} = Yaw_d - Yaw_0 \tag{3}$$

Preprints (www.preprints.org) | NOT PEER-REVIEWED | Posted: 4 July 2023 doi:10.20944/preprints202307.0027.v1



Where, is the installation error of the dual antenna, is the average of the recorded heading angle of the dual antenna.

Therefore, the real time true heading angle of the farm machinery is：

$$Yaw = Yaw_1 + E_{Yaw} \tag{4}$$

where $Yaw$ is the real time true heading of the farm machine and $Yaw_1$ is the real time collected heading of the farm machine.

（2）Automatic calibration of roll angle and pitch angle

Adopt the way of round-trip straight-line driving of the agricultural machine under the same path, i.e. driving along the same path in the positive direction and driving in the negative direction once each. When driving in the positive direction, the value of the positive direction travel traverse angle and the value of the pitch angle are recorded, and when driving in the opposite direction, the value of the reverse direction travel traverse angle and the value of the pitch angle are recorded. Half of the average value of the round-trip traverse angle is the installation deviation angle of the sensor relative to the traverse angle of the vehicle body, as shown in Equation (5); Similarly, half of the average value of the round-trip pitch angle is also the installation deviation angle of the sensor relative to the vehicle body pitch angle, as shown in Equation (6).

$$E_{roll}=-\left(\frac{\frac{\sum_{i=1}^{n} roll\text{-}P_i}{n}+\frac{\sum_{i=1}^{n} roll\text{-}N_i}{n}}{2}\right)=-\frac{(roll\text{-}P_1+roll\text{-}P_2+\cdots roll\text{-}P_n)+(roll\text{-}N_1+roll\text{-}N_2+\cdots roll\text{-}N_n)}{2n} \tag{5}$$

Where, $E_{roll}$ is the roll angle measurement error; $roll\text{-}P_i$ is the i-th roll angle value of the positive direction of travel, $n$ is the sample capacity; $roll\text{-}N_i$ is the i-th roll angle value of the negative direction of travel.

$$E_{pitch}=-\left(\frac{\frac{\sum_{i=1}^{n} pitch\text{-}P_i}{n}+\frac{\sum_{i=1}^{n} pitch\text{-}N_i}{n}}{2}\right)=-\frac{(pitch\text{-}P_1+pitch\text{-}P_2+\cdots pitch\text{-}P_n)+(pitch\text{-}N_1+pitch\text{-}N_2+\cdots pitch\text{-}N_n)}{2n} \tag{6}$$

Where, $E_{pitch}$ is the pitch angle measurement error; $pitch\text{-}P_i$ is the i-th pitch angle value of the positive direction travel, $n$ is the sample capacity; $pitch\text{-}N_i$ is the i-th pitch angle value of the negative direction travel.

Therefore, the real time true roll angle of the agricultural machine is:

$$roll = roll_1 + E_{roll} \tag{7}$$

Where, $roll$ is the real time real time roll angle of the farm machine, $roll_1$ is the real time collected roll angle of the farm machine.

The real time true pitch angle of the farm machinery is:

$$pitch = pitch_1 + E_{pitch} \tag{8}$$

Where, $pitch$ is the real time true pitch angle of the farm machine, $pitch_1$ is the real time pitch angle of the farm machine.

2.2.2. Outlier rejection

In order to ensure the integrity of the collected hard-bottom contour information and intelligent agricultural machine operation data, the data acquisition module of the unmanned system sets 50 Hz acquisition frequency for data acquisition of sensor information and real-time parameters of the operation, and the data frames are prone to anomalies and incomplete data preservation due to the

Preprints (www.preprints.org) | NOT PEER-REVIEWED | Posted: 4 July 2023 doi:10.20944/preprints202307.0027.v1



large amount of data and when the system needs to start and stop due to special circumstances during the operation, resulting in ghost points during the acquisition process [29]. Such anomalies occur in the attitude sensor data acquisition process, where there are more coarse points of anomalous values in the transverse roll angle and pitch angle acquisition, and these are observed from the timing samples, and these points show abnormally large deviations in the data in the longitudinal axis direction, so that the rear wheel bottom trajectory and the constructed hard-bottom contour will show sharp protrusions in the constructed hard-bottom contour, which cannot accurately express the true hard-bottom contour characteristics. In order to avoid the influence of anomalies to the hard-bottom contour feature extraction, this study adopts the Lajda criterion to remove the outliers from the raw data of the attitude sensor transverse roll angle and pitch angle measurements. The principle is to first assume that a set of detection data contains only random errors, to calculate and process them to obtain the standard deviation σ, and then set the probability interval to which the confidence value belongs, and consider the errors beyond this interval as suspicious data, which is set as [-3σ, 3σ], and the data beyond this error should be removed.

The measurement of roll angle and pitch angle are both continuous measurements with equal precision, and the anomalies are rejected separately by setting the measurement data set as $\{X_1, X_2, \cdots, \mathrm{X}_i\}(i = 1, 2, \cdots, n)$ and $M$ as their respective arithmetic averages. $M$ is calculated as shown in Equation (9); the standard deviation σ is calculated according to Bessel's formula as shown in Equation (10); if a measurement value $\mathrm{X}_i$ satisfies Equation (11), the point is considered as a rough point and is rejected. is rejected.

$$M = \frac{\sum_{i=1}^{n} X_i}{n} = \frac{X_1 + X_2 + \cdots \mathrm{X}_N}{n} \tag{9}$$

$$\sigma = \sqrt{\frac{1}{n}\sum_{i=1}^{n}(X_i - M)^2} \tag{10}$$

$$|X_i - M| > 3\sigma \tag{11}$$

2.2.3 Contour trajectory 3D spline curve denoising

Since the positioning error of RTK-GNSS positioning system in elevation is 1.5cm+1ppm, the raw data of the hard-bottom contour trajectory collected by the rear wheels of the farm machinery is continuously "sawtooth" on the temporal chart, and when the intelligent farm machinery encounters unexpected situation during operation that causes stopping or very small speed, according to the emergence of suspended the representative contour trajectory of the operation (Figure 2a) can be seen that the 3D spline curve of the trajectory composed of the collected contour points is prone to self-crossing and two points overlap, as shown in Figure 2b. The actual contour should be a continuous spline curve contour, and there is no self-crossing in the front and back spatial point connection, so the real hard bottom local contour 3D spline trajectory line is obtained by sliding denoising of the collected raw data without affecting the acquisition accuracy. Therefore, in this paper, moving average and wavelet denoising [30] are used for the comparative analysis of local acquisition contour processing, and the results are shown in Figure 2.

Preprints (www.preprints.org) | NOT PEER-REVIEWED | Posted: 4 July 2023 doi:10.20944/preprints202307.0027.v1



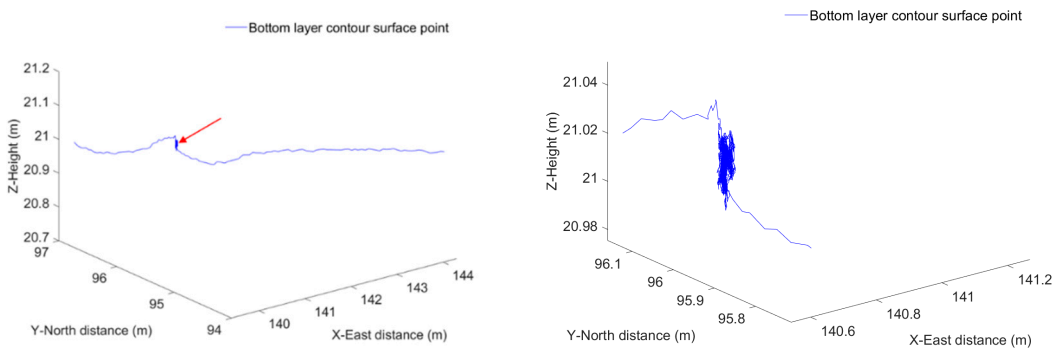


(a) (b)

Figure 2. Repeated and self-intersecting sets of points on job suspension: (a) Representative contour trajectory; (b) Continuous acquisition at the same position when the operation is suspended.

According to the processing results in Figure 3 above, we can see that although the moving average filtering can remove the " sawtooth" noise of the hard bottom contour, but the cost is that the original contour details are lost, such as the original contour has mutation and texture, the mean filtering will make these details lost, the hard bottom contour will become too smooth, as shown in Figure 3a. The wavelet has the advantage of multi-resolution analysis, for the analysis of hard bottom contour features such as non-smooth signal, in the case of contours with edges or elevation abrupt changes, the wavelet can be decomposed to different resolutions (scales) to deal with them separately, as shown in Figure 3b. That is to remove the "sawtooth" noise and self-phase intersection set of the hard-bottom contour, but also to ensure the authenticity of the processed hard-bottom local contour elevation abrupt changes or edge information, so as to obtain a 3D spline curve of the local contour trajectory.

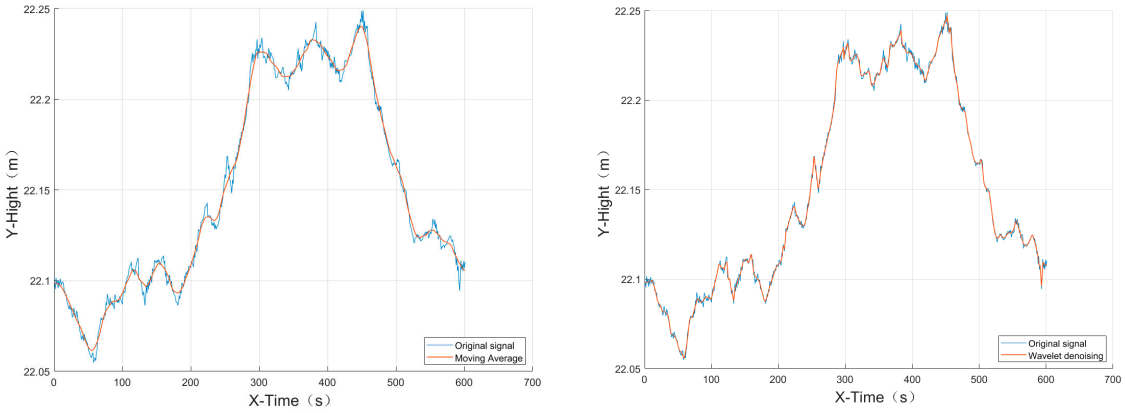


(a) (b)

Figure 3. Moving average denoising and wavelet denoising are compared: (a) Moving average denoising; (b) Wavelet denoising.

*2.3 Hard bottom layer surface roughness estimation method*

In order to quickly and continuously measure the hard substrate roughness of the intelligent farm machine traveling in real time, this section takes the hard substrate profile within the set length as the local roughness measurement range, that is, the hard substrate roughness measured by the farm machine at each moment is the roughness value measured from the previous moment to the set length of the moment traveling, and the sampling method is shown in Figure 4. The uniform operating speed and data collection frequency set by the intelligent farm machine are known, then the total number of data frames from the previous moment to the present moment can be calculated, and the calculation formula is shown in Equation (12).

Preprints (www.preprints.org) | NOT PEER-REVIEWED | Posted: 4 July 2023 doi:10.20944/preprints202307.0027.v1



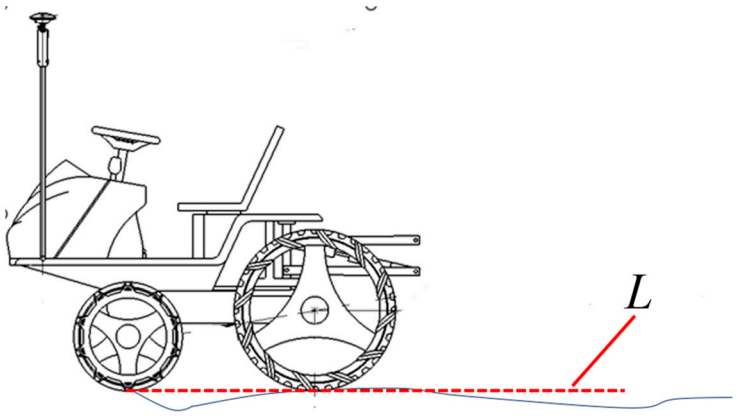


**Figure 4.** Sampling diagram.

$$n_z = L / v * f \tag{12}$$

where $n_z$ is the number of data frames from a previous moment to the present moment, $L$ is the sampling length, m; $v$ is the operating speed, m/s; and $f$ is the acquisition frequency, Hz.

Based on the hard bottom contour information collected from the intelligent farm machine chassis, a straight line is fitted based on the least squares index method within a locally set length range, and the height of each point from this fitted line is calculated to provide input for calculating the surface roughness. The method can be applied to both flat and sloping land, and the hard bottom contour, local fitted line segment and contour point to fitted straight line height relationship diagrams in flat and sloping land are shown in Figure 5a and Figure 5b, respectively.

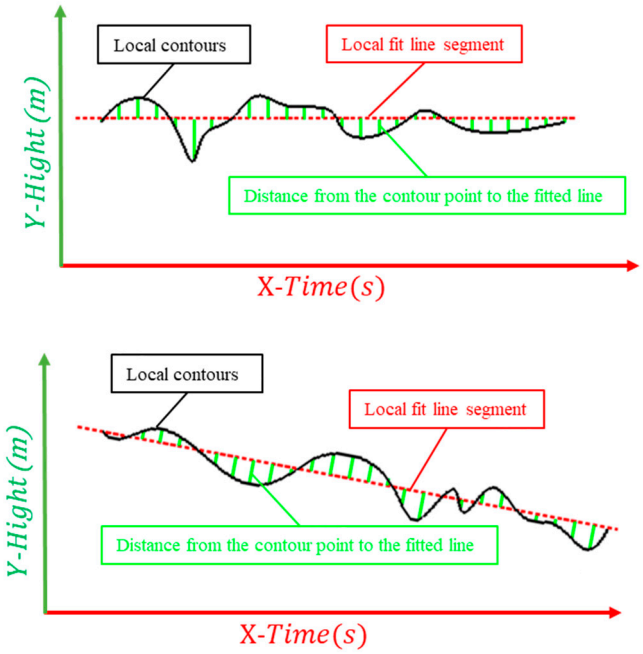


(a) (b)

**Figure 5.** Hard-bottom contour, local fit line segment and contour point-to-fit straight line height relationship diagram: (**a**) Flat land; (**b**) Sloping land.

Let the expression of the locally fitted straight line based on the least squares fit be:

$$y_1 = Ax_1 + B \tag{13}$$

Preprints (www.preprints.org) | NOT PEER-REVIEWED | Posted: 4 July 2023 doi:10.20944/preprints202307.0027.v1



Where, $y_1$ is the height value of the upper point of the fitted line, $x_1$ is the contour point number value, $A$ is the slope of the fitted line, and $B$ is the intercept of the fitted line.

Let the distance of the i-th contour point in the local range to the fitted straight line be $S_i$, then we have:

$$S_i = \frac{|A * n_i - z_i + B|}{\sqrt{A^2 + B^2}} \tag{14}$$

Where, $S_i$ is the distance from the i-th contour point to the fitted line; $n_i$ the i-th contour point serial number; $z_i$ is the i-th contour point height.

Then let the local surface roughness at the j-th point of the hard bottom layer be $R_{d_j}$, calculated as follows:

$$R_{d_j} = \frac{1}{n_z}\int_0^{n_z} |S| dx \tag{15}$$

Since the collected hard bottom layer is a discrete point then it can be approximated as:

$$R_{d_j} = \frac{1}{n_z}\sum_{i=1}^{n_z} |S_i| \tag{16}$$

According to Equation 16, the local surface roughness characteristics of the hard bottom contour of the whole area of the farm machinery can be obtained by traversing the hard bottom layer collected from the whole area of operation.

## 3. Results

### *3.1. Test scenario*

The paddy hard bottom layer contour sensing module was integrated into the unmanned system of agricultural machinery, and the unmanned rice direct seeding machine was used to perform unmanned mechanical seeding operation and collect the paddy hard bottom layer contour in the rice unmanned farm in Zengcheng District, Guangzhou City, South China Agricultural University. The planned operation path of the direct seeding machine is shown in Figure 6a, and the operation site is shown in Figure 6b.

(**a**) (**b**)

**Figure 6.** Unmanned seeder planning operation path and site: (a) Planned operational path; (b) Operational site.

The heading angle calibration was carried out in the straight-line driving section of the unmanned agricultural machine, and the automatic calibration method of heading angle was

Preprints (www.preprints.org) | NOT PEER-REVIEWED | Posted: 4 July 2023 doi:10.20944/preprints202307.0027.v1



adopted in Section 2.2.1. The results of the line model constructed by fitting the trajectory of the main positioning antenna for straight-line driving are shown in Figure 7, Equation (17) and Table 1.

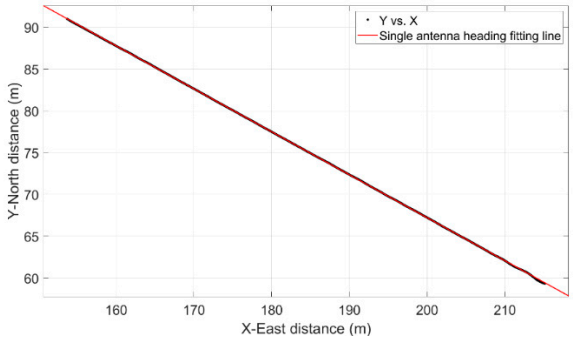


**Figure 7.** Unmanned seeder driving in a straight line main antenna position fitting straight line.

$$y = -0.5146x + 170.1 \tag{17}$$

**Table 1.** Linear fit of single antenna heading angle.

| Sample size | R-square | RMSE | SSE | Adj R-sq |
|---|---|---|---|---|
| 16135 | 1 | 0.0099 | 1.5761 | 1 |

According to the linear fitting model of single antenna heading angle, the slope $k$ is -0.5146, and according to equation 2, the true heading angle of the car body $Yaw_d$ is 152.77°, and the recorded heading average of the dual antenna $Yaw_0$ is 151.0711°, and according to equation 3, the fixed installation deviation of the dual antenna and the car body $E_{Yaw}$ is 1.6989°, so according to equation 4, the true heading angle of the car body $Yaw$ is the dual satellite antenna heading angle measurement value $Yaw_1$ plus 1.6989°.

The automatic calibration of the roll angle and pitch angle was carried out in the unmanned seeder round-trip transport straight-line driving section, and the farm machine was driven once along the same path in the positive direction and once in the negative direction, and the automatic calibration method of the roll angle and pitch angle in Section 2.2.1 was adopted, and the recorded rear wheel trajectory diagrams were shown in Figure 8a and Figure 8b, respectively, and the average values of the collected roll angle and pitch angle and calculated according to Equations (5) and (6). The obtained measurement error results are shown in Table 2.

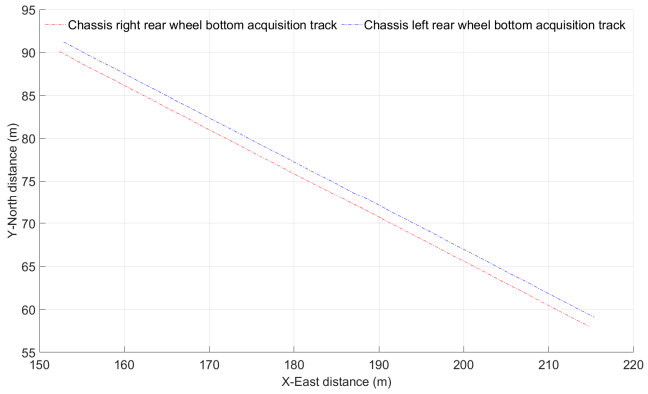


(**a**)

Preprints (www.preprints.org) | NOT PEER-REVIEWED | Posted: 4 July 2023 doi:10.20944/preprints202307.0027.v1



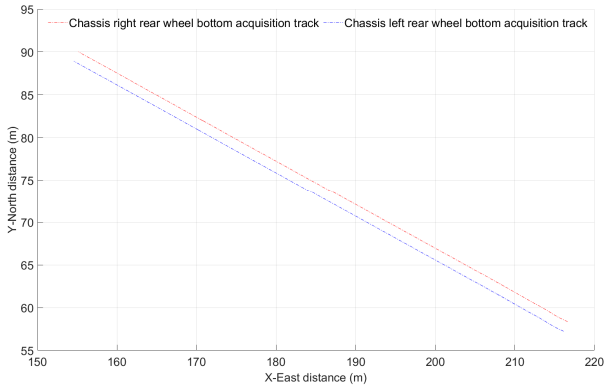


(**b**)

**Figure 8.** Round-trip linear trajectory under the same path: (**a**) Forward travel trajectory; (**b**) Reverse travel trajectory.

**Table 2.** The mean and error of the cross-roll angle of round-trip straight driving and driving cross-roll angle.

| | **Roll Angle/°** | **Pitch angle/°** |
|---|---|---|
| Average value (driving in positive direction) | 0.197435 | -3.11529 |
| Average value (driving in opposite direction) | -0.27745 | -1.0474 |
| Sensor mounting error | 0.04001 | 2.08134 |

According to Equations (7) and (8) and Table 2, it is known that the real time true roll angle $roll$ of the farm machine is the real time collected roll angle $roll_1$ of the farm machine plus 0.04 degrees, and the real time true pitch angle $pitch$ of the farm machine is the real time collected pitch angle $pitch_1$ plus 2.08 degrees.

In the total 772013 data acquisition, the outliers of the roll angle acquisition occurred 22 times non-continuously and irregularly, and the outliers of the pitch angle acquisition occurred 48 times non-continuously and irregularly. Using the outlier rejection method in Section 2.2.3, the results of roll angle and pitch angle acquisition before and after the outlier rejection are shown in Figure 9; the constructed rear wheel bottom trajectory and constructed hard bottom profile before and after the outlier rejection are shown in Figure 10.

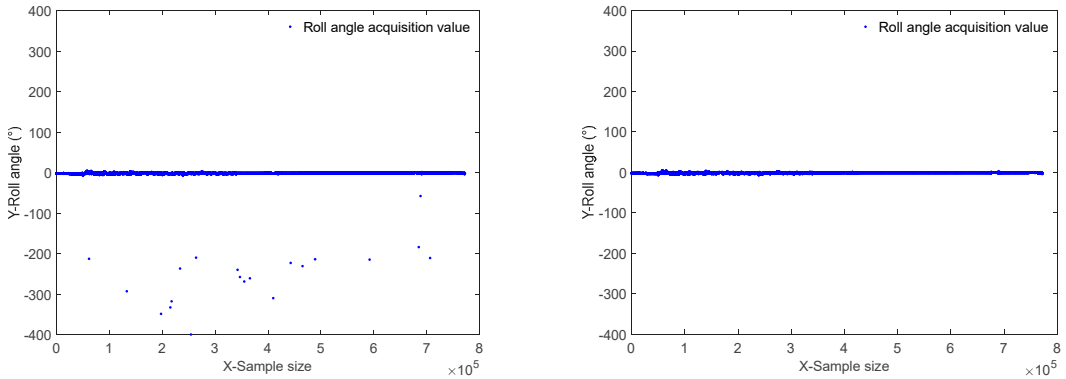


(**a**) (**b**)

Preprints (www.preprints.org) | NOT PEER-REVIEWED | Posted: 4 July 2023 doi:10.20944/preprints202307.0027.v1



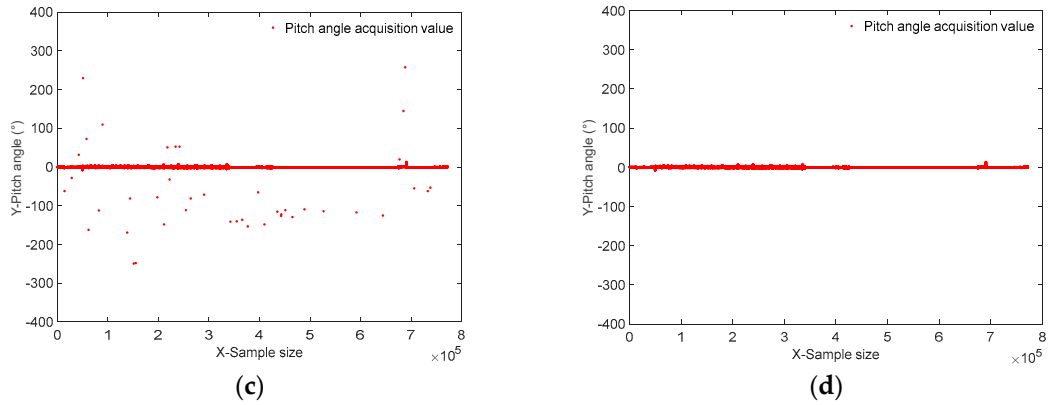


**Figure 9.** Attitude sensor acquisition value set: (**a**) The original set of values for roll angle acquisition; (**b**) The set of values for roll angle acquisition after removing outliers; (**c**) Original set of values for pitch angle acquisition; (**d**) Set of values for pitch angle acquisition after rejecting outliers.

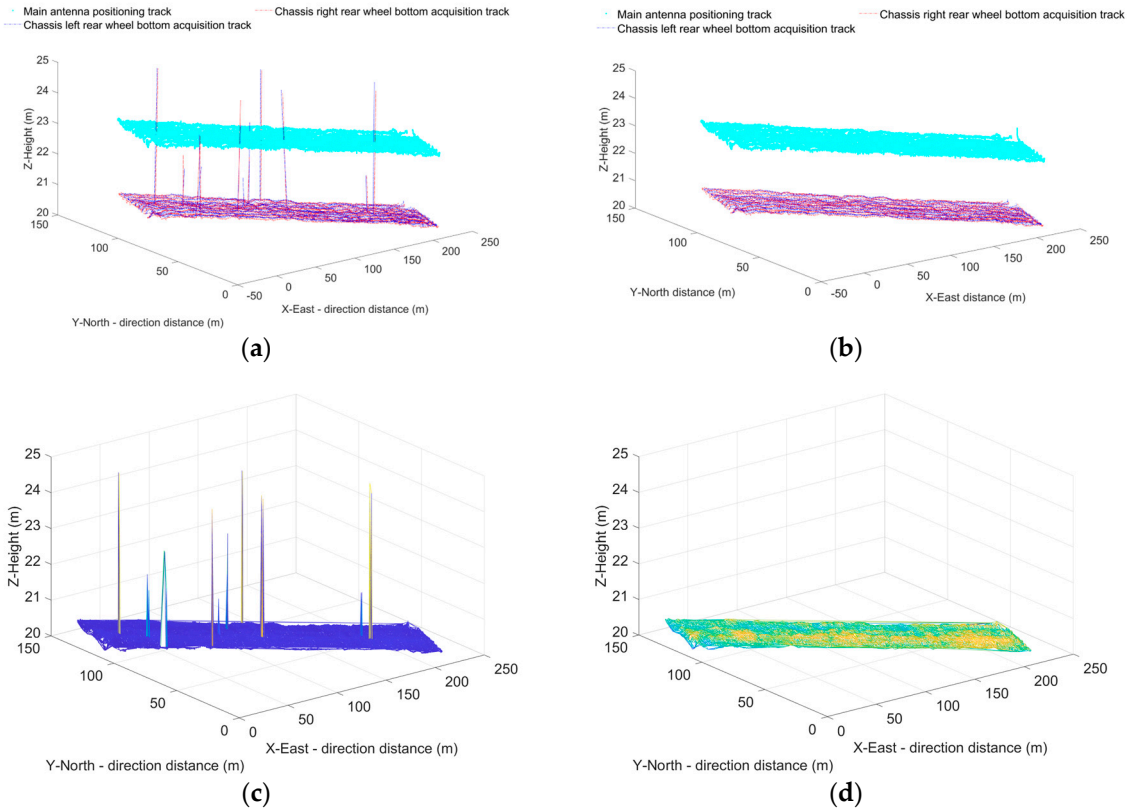


**Figure 10.** Rear wheel bottom track with hard bottom profile: (**a**) Initial wheel track collected from the rear wheel bottom; (**b**) Rear wheel bottom track after removing anomalies; (**c**) Acquisition of the initial hard bottom contour; (**d**) Hard bottom contour after removal of outliers.

### *3.2. Quantitative estimation of hard bottom profile roughness characteristics for whole fields*

The hard bottom surface roughness estimation method is used to estimate the whole field block, and the estimated hard bottom contour surface roughness eigenvalues are associated with the positioning information, and the digital model of the whole field local roughness is constructed as shown in Figure 11. The digital model can provide speed control reference basis for the intelligent farm machine, that is, the larger the feature value indicates the rougher the local surface of the hard substrate layer, and it is recommended to reduce the operation speed accordingly in this position to ensure the operation quality; the smaller the feature value indicates that the hard substrate layer for operation driving is relatively flat, and it is recommended to increase the operation speed accordingly

Preprints (www.preprints.org) | NOT PEER-REVIEWED | Posted: 4 July 2023 doi:10.20944/preprints202307.0027.v1



in this position to improve the operation efficiency, so as to improve the operation speed and operation quality of the intelligent farm machine as a whole.

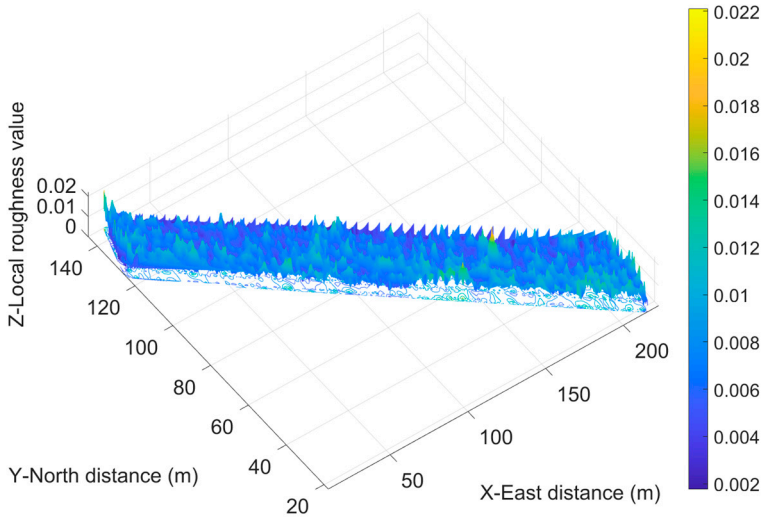


**Figure 11.** Digital feature model of local roughness of whole field.

The distribution of local roughness values was analyzed according to the whole-field local roughness digital characteristic model, and the results are shown in Figure 12. The mean value of the whole-field local roughness of the test water field was 0.0065, and 68.27% of the local roughness values were distributed in the interval of [0.0042,0.0087], and 99.73% were distributed in the interval of [0,0.0133]. In addition, the higher frequency of measured local roughness in the interval [0.0008,0.002] is due to the longer idle stopping time and repeated acquisition at the same location.

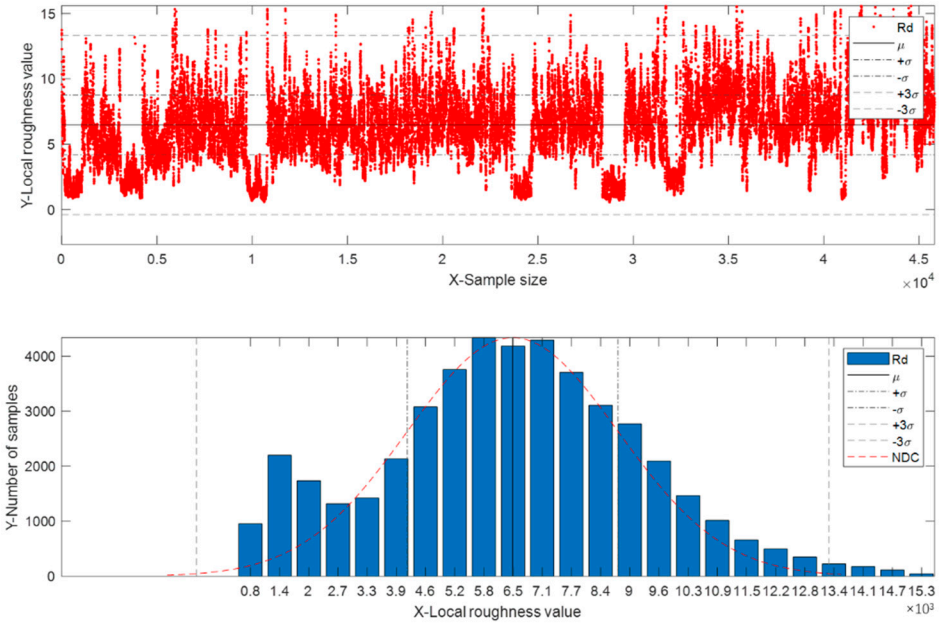


**Figure 12.** Distribution of local roughness in the whole field.

*3.3 Representative hard bottom contour surface characterization*

According to the unmanned seeder heading angle change characteristics and the corresponding driving trajectory, the representative driving route from the hangar to the field containing

Preprints (www.preprints.org) | NOT PEER-REVIEWED | Posted: 4 July 2023 doi:10.20944/preprints202307.0027.v1



transportation, down-field, operation and trapping, etc. is selected, and the roughness characteristics of different hard bottom contours of agricultural machine driving are analyzed, where "①" is marked with the straight downhill driving section of cement road. "②" is marked with the idle stop section. "③" is marked with the straight driving section on the flat cement road. "④" is marked with the section of driving into the entrance of the field. "⑤" is marked as the normal straight line driving operation section of the paddy field, and"⑥" is marked with the section of trapped vehicles. The route of the car body heading changes shown in Figure 13, the trajectory as shown in Figure 14.

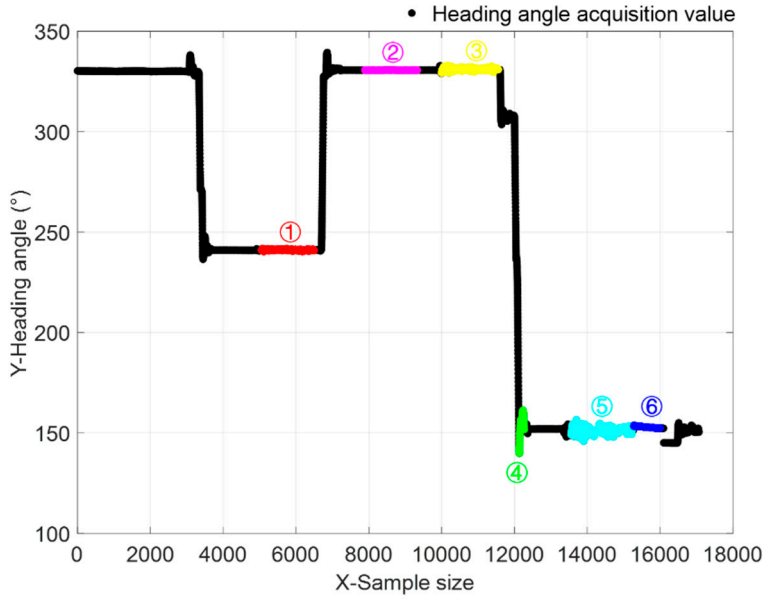


**Figure 13.** Hangar-to-field transport and field operation heading angle of unmanned seeder.

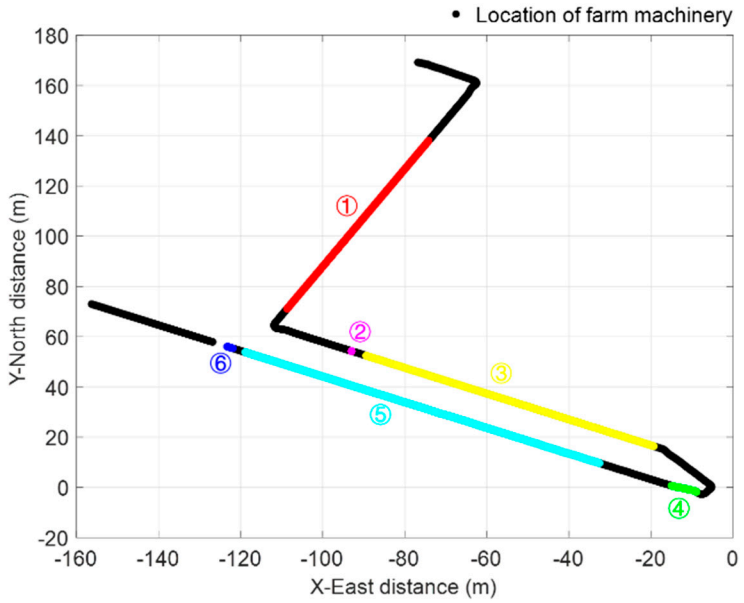


**Figure 14.** Hangar-to-field transport and field operation trajectory of unmanned seeder.

Based on the hard bottom sliding surface roughness estimation method, calculate the hard bottom local surface roughness of each driving section respectively , the whole 6 cases of driving hard bottom local surface roughness characteristics as shown in Figures 15 and 16 and Table 3. According to the measured roughness results of each driving segment, it can be seen that the smart farm machine in the idle state, due to the wheel bottom measurement elevation out of the measurement error no

Preprints (www.preprints.org) | NOT PEER-REVIEWED | Posted: 4 July 2023 doi:10.20944/preprints202307.0027.v1



elevation change, the measured surface roughness value is the lowest 0.0011; followed by the road surface roughness 0.0023 collected on the flat and straight cement road is less than 0.0037 collected on the straight downhill cement road; the surface roughness of the water field operation segment is greater than the cement road for 0.007; in the inlet section, because of the transition from dry paddy to wet paddy, the contour elevation difference is larger, so the surface roughness measured in this section is 0.0951 larger than the roughness of normal operation in paddy; and in the trap section, because of the local appearance of hard bottom contour elevation drops sharply, the measured roughness value is the largest 0.1236.

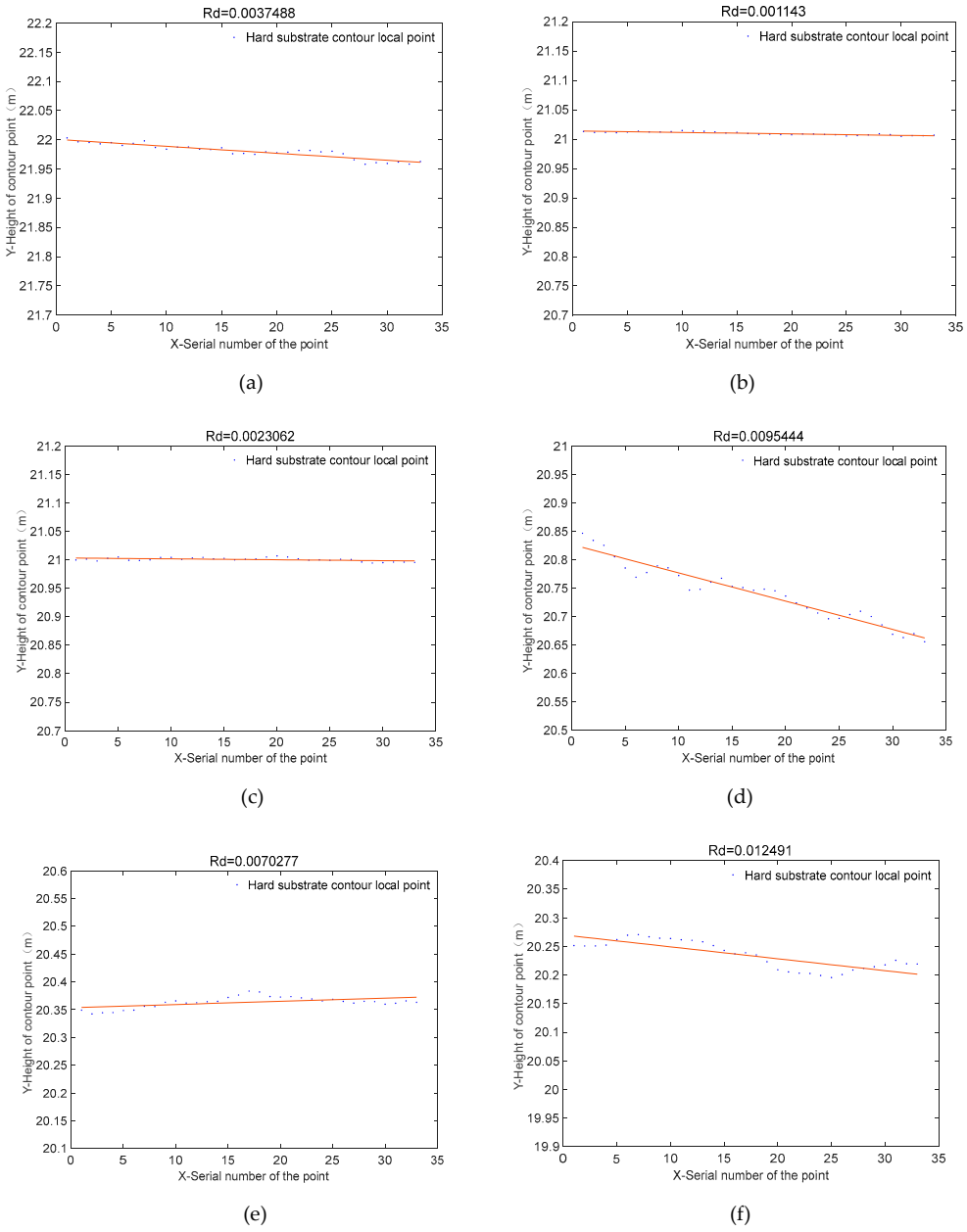


**Figure 15.** Surface roughness characteristics of transport, down-field, operation and trapping links: (a) ①-Concrete road on downhill slope; (b) ②-Stop idling; (c) ③-flat concrete pavement; (d) ④-paddy field inlet; (e) ⑤-Water field operation; (f) ⑥-Trap section.

Preprints (www.preprints.org) | NOT PEER-REVIEWED | Posted: 4 July 2023 doi:10.20944/preprints202307.0027.v1



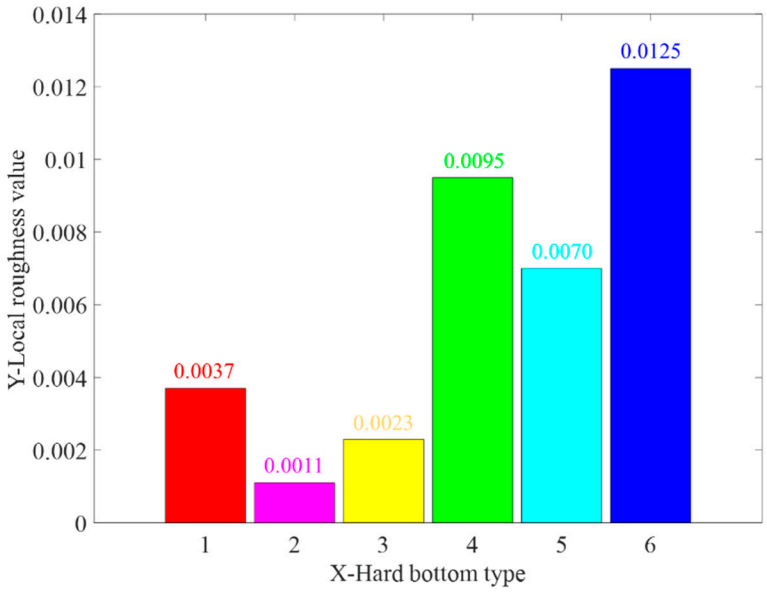


**Figure 16.** Representative driving section surface roughness.

**Table 3.** Representative driving section surface roughness value.

| No. | ① | ② | ③ | ④ | ⑤ | ⑥ |
|---|---|---|---|---|---|---|
| Starting point number | 5056 | 7893 | 10000 | 12126 | 14782 | 15280 |
| Termination point number | 6496 | 9329 | 11557 | 12268 | 15229 | 16001 |
| Rd | 0.0037 | 0.0011 | 0.0023 | 0.0095 | 0.0070 | 0.0125 |

When the intelligent agricultural machine drives on different road sections to collect hard bottom contours, the stepless classification of road conditions in different situations is realized according to the variability of local surface roughness values, which can provide a reference basis for unmanned system vehicle motion control.

## 4. Discussion

It is of great significance to study the method of quantifying the local characteristics of the hard bottom contour of intelligent agricultural machine driving and analyze the local hard bottom condition of intelligent agricultural machine unmanned operation driving, so as to provide real-time driving environmental feedback for intelligent agricultural machine and realize the precise and high quality and efficient operation of agricultural machine unmanned.

This paper addresses the problem that it is difficult to quantify and express the local features of hard bottom layer of paddy fields driven by unmanned operation of intelligent farming machines, and proposes a method to quantify the local features of hard bottom layer contour of intelligent farming machine driving by taking unmanned direct seeding machine equipped with GNSS and AHRS as the hard bottom layer contour sensing platform, and realizes automatic calibration of position and attitude sensors of intelligent farming machine, which reduces the sensor installation precision requirements and calibration difficulties; In view of the problem that the unmanned system collects data prone to flypoints, it realizes the rejection of abnormal values of the collected hard-bottom layer data, constructs a global roughness distribution model with associated position information based on the acquired hard-bottom layer contour data, and obtains the surface roughness feature quantity at any position of the field, which can provide environmental feedback parameters for the unmanned operation of intelligent farming machines and provide reference for the adaptive speed control of intelligent farming machines and the improvement of operation quality and

operation efficiency. The variability of contour features under the automatic transfer route from the hangar to the field of the unmanned operation of intelligent farm machinery is analyzed, which can provide a basis for the unmanned operation of intelligent farm machinery to set the operation and control parameters to improve the operation efficiency by segments.

The method designed in this paper, for the convenience of mechanical structure transformation design, the contour sensing platform uses the position measurement sensor installed on the original mechanism of the waterfield agricultural machine, there is a small vibration of the positioning antenna in the bumpy environment, if the installation structure stiffness and installation accuracy can be improved, can further improve the measurement accuracy and reduce the sensor position correction steps; In this paper, the hard bottom layer contour acquisition in paddy field adopts the intelligent farm machine fixed speed 0.65m/s and the specific length 2m range to extract the local contour, which can distinguish the characteristics of different hard bottom layer contours, and if the speed of intelligent farm machine can be correlated, the corresponding length range contour can be adaptively selected for contour feature extraction under different speed, which can further improve the adaptability of different farm machines; in addition, the method in this paper is based on In addition, the method in this paper is based on hard bottom contour digital modeling to calculate the local features of the whole area, which is a large amount of calculation, and the background calculation is used. This is also one of our future research directions.

## 5. Conclusions

The hard bottom layer of the paddy field where the unmanned operation of intelligent farming machine is running is complex with different potholes, which has a greatimpact on the driving stability and operation quality and efficiency of intelligent farming machine. It is difficult to ensure the stability of unmanned operation path tracking control of intelligent farm machines operating under fields with large differences in hard bottom layer contour characteristics; The sensor installation position of the hard substratum sensing platform is random, and the collected data are prone to flypoints, which makes it difficult to realize the continuous quantitative expression of the local features of the hard substratum of paddy fields, increasing the difficulty of analyzing the contour features of the hard substratum of paddy fields and the lack of quantitative expression methods of the local features of the hard substratum of paddy fields. In view of the above problems, this paper carries out the method and experimental research on the quantification of local features of hard substratum contour of intelligent farm machinery driving. It mainly includes:

(1) The data processing methods of automatic calibration of sensor installation error, outlier rejection and 3D spline curve denoising of contour trajectory are designed. The real heading angle is obtained by obtaining the trajectory of the main positioning antenna of the intelligent farm machine in a straight line and fitting it to a straight line, and the difference is calculated and compensated by comparing it with the installed dual antenna directional acquisition heading angle to realize the heading calibration; The system error of round-trip roll angle and pitch angle is obtained by using the round-trip straight-line driving of the intelligent farm machine under the same path, and the calibration of roll and pitch angle is realized; the raw data processing of sensor measurement by using the Lajda criterion and wavelet denoising method, and the rejection of hard bottom contour ghost points and intersection points is realized by the intelligent farm machine collection.

(2) The quantification method of local features of hard bottom layer was established. Based on the field operation of unmanned live broadcasters and simultaneous collection of hard bottom layer information, the local feature quantification of hard bottom layer of paddy fields with correlated location information was achieved by using the method of calculating local sliding surface roughness to evaluate the degree of hard bottom layer surface bumps. The quantified local characteristics of hard bottom layer in the test plots showed that the mean value of local roughness was 0.0065, 68.27% was distributed in the interval of [0.0042, 0.0087], and 99.73% was distributed in the interval of [0,0.0133].

(3) The surface roughness variability of representative driving sections was analyzed. The hard bottom surface profile feature evaluation method based on local sliding surface roughness analyzes

the hard bottom surface roughness features of representative driving routes such as intelligent agricultural machinery unmanned operation transport, down field, operation and trapping, compares the representative driving section profile feature variability based on local surface roughness, and proves the feasibility of the quantification method of local features of hard bottom layer.

The method of quantifying hard-bottom local features of intelligent agricultural machines driving can provide feedback on the local environmental features of their unmanned operation at the current location of driving, and provide a reference basis for the optimization of unmanned systems designed to improve the efficiency and quality of intelligent agricultural machine operations.

**Author Contributions:** Conceptualization, T.T., L.H., X.L. and J.H.; methodology, T.T., L.H., X.L. and J.H.; software, T.T., L.T., G.C., W.C., M.L. and Y.L.; validation, T.T., Z.M., D.F., K.H. and L.Z.; formal analysis, T.T.; investigation, T.T. and Y.L.; resources, T.T., L.H., X.L., J.H. and P.W.; data curation, T.T., L.H. and J.H.; writing—original draft preparation, T.T.; writing—review and editing, T.T., L.H., X.L. and J.H.; visualization, T.T., L.H., P.W. and M.Y.; supervision, L.H., X.L. and J.H.; project administration, X.L.; funding acquisition, X.L., L.H. and J.H.. All authors have read and agreed to the published version of the manuscript.

**Funding:** This research was funded by the National Key Research and Development Program of China (Grant No.2021YFD2000602), the Jiangxi Provincial Science and Technology Special Project of Jinggangshan Agricultural High-tech Zone (Grant No.20222-051252), and the National Natural Science Foundation of China (Grant No.32071913; No.32101623).

**Data Availability Statement:** The data that supports this study will be shared upon reasonable request to the corresponding author.

**Acknowledgments:** We would like to thank the our partners of Zengcheng Teaching Base of South China Agricultural University for their help and support in field management and machine maintenance.

**Conflicts of Interest:** The authors declare no conflict of interest.Grant No.

## References

1. Nawaz, A., Rehman, A. U., Rehman, A., Ahmad, S., Siddique, K. H. M., and Farooq, M. Increasing sustainability for rice production systems. *Journal of Cereal Science* **2022**, *103*, 103400, doi:10.1016/j.jcs.2021.103400.
2. Kuenzer, C., and Knauer, K. Remote sensing of rice crop areas. *International Journal of Remote Sensing* **2013**, *34*, 2101-2139, doi:10.1080/01431161.2012.738946.
3. Xin, F., Xiao, X., Dong, J., Zhang, G., Zhang, Y., Wu, X., Li, X., Zou, Z., Ma, J., Du, G., Doughty, R. B., Zhao, B., and Li, B. Large increases of paddy rice area, gross primary production, and grain production in Northeast China during 2000–2017. *Science of The Total Environment* **2020**, *711*, 135183, doi:10.1016/j.scitotenv.2019.135183
4. Zhao, Y. Statistical analysis of the changes of cultivated land resources in the past 10 years. Territ. *Nat. Resour. Study* **2020**, *1*, 53-57, doi:10.16202/j.cnki.tnrs.2020.01.013
5. Chengliang, L., Hongzhen, L., Yanming, L., Liang, G., and Zhonghua, M. Analysis on status and development trend of intelligent control technology for agricultural equipment. *Nongye Jixie Xuebao/Transactions of the Chinese Society of Agricultural Machinery* **2020**, *51*, doi:10.6041/j.issn.1000-1298.2020.01.001
6. Xuegeng, C., Haojun, W., Weirong, Z., Fochu, P., and Yan, Z. Advances and progress of agricultural machinery and sensing technology fusion. *Smart Agriculture* **2020**, *2*, 1, doi:10.12133/j.smartag.2020.2.4.202002-SA003
7. Luo, X., Liao, J., Zang, Y., Ou, Y., and Wang, P. Developing from Mechanized to Smart Agricultural Production in China. *Strategic Study of Chinese Academy of Engineering* **2022**, *24*, 46-54, doi: 10.15302/J-SSCAE-2022.01.005
8. Luo, X., Liao, J., Hu, L., Zhou, Z., Zhigang, Z., Zang, Y., Wang, P., and He, J. Research progress of intelligent agricultural machinery and practice of unmanned farm in China. *Journal of South China Agricultural University* **2021**, *42*, 8-17, doi:10.7671/j.issn.1001-411X.202108040
9. He, J., Hu, L., Wang, P., Liu, Y., Man, Z., Tu, T., Yang, L., Li, Y., Yi, Y., Li, W., and Luo, X. Path tracking control method and performance test based on agricultural machinery pose correction. *Computers and Electronics in Agriculture* **2022**, *200*, 107185, doi:10.1016/j.compag.2022.107185
10. Hu, L., Luo, X., Lin, C., Yang, W., Xu, Y., and Li, Q. Development of 1PJ-4.0 laser leveler installed on a wheeled tractor for paddy field. *Nongye Jixie Xuebao= Transactions of the Chinese Society for Agricultural Machinery* **2014**, *45*, 146-151, doi:10.6041/j. issn.1000-1298.2014.04.023

11. Li, H., Niu, D., Wang, Y., Li, X., Meng, Q., and Liu, G. Rapid survey technology of farmland terrain based on RTK-GNSS. *Journal of China Agricultural University* **2014**, *19*, 188-194, doi:10.11841/j.issn.1007-4333.2014.06.26
12. Hu, L., Yang, W., Xu, Y., Zhou, H., Luo, X., Ke, X., and Zi, S. Design and experiment of paddy field leveler based on GPS. *Journal of South China Agricultural University* **2015**, *36*, 130-134, doi:10.7671/j.issn.1001-411X.2015.05.022
13. Gang, L., Xiao, L., Xi, K., Youxiang, X., and Dongling, N. Automatic Navigation Path Planning Method for Land Leveling Based on GNSS. *Nongye Jixie Xuebao/Transactions of the Chinese Society of Agricultural Machinery* **2016**, doi:10.6041/j.issn.1000-1298.2016.SO.004
14. Youxiang, X., Gang, L., Xi, K., and Yunpeng, J. Optimization and Analysis of Location Accuracy Based on GNSS-controlled Precise Land Leveling System. *Nongye Jixie Xuebao/Transactions of the Chinese Society of Agricultural Machinery* **2017**, doi:10.6041/j.issn.1000-1298.2017.SO.007
15. Rovira-Más, F., Zhang, Q., and Reid, J. F. Stereo vision three-dimensional terrain maps for precision agriculture. *Computers and Electronics in Agriculture* **2008**, *60*, 133-143, doi:10.1016/j.compag.2007.07.007
16. Marinello, F., Pezzuolo, A., Gasparini, F., Arvidsson, J., and Sartori, L. Application of the Kinect sensor for dynamic soil surface characterization. *Precision agriculture* **2015**, *16*, 601-612, doi:10.1007/s11119-015-9398-5
17. Yandun Narváez, F., Gregorio, E., Escolà, A., Rosell-Polo, J. R., Torres-Torriti, M., and Auat Cheein, F. Terrain classification using ToF sensors for the enhancement of agricultural machinery traversability. *Journal of Terramechanics* **2018**, *76*, 1-13, doi:10.1016/j.jterra.2017.10.005
18. ZHANG, M., CHEN, Y., JIA, W., and Wang, M. Design of three dimensional topographic information measuring system [J]. *Journal of Jilin University (Engineering and Technology Edition)* **2007**, *37*, 1451-1454, doi:10.13229/j.cnki.jdxbgxb2007.06.049
19. Starek, M. J., Chu, T., Mitasova, H., and Harmon, R. S. Viewshed simulation and optimization for digital terrain modelling with terrestrial laser scanning. *International Journal of Remote Sensing* **2020**, *41*, 6409-6426, doi:10.1080/01431161.2020.1752952
20. Tu, T., He, J., Luo, X., Hu, L., Wang, P., Chen, G., Tian, L., Feng, D., Wang, Z., Man, Z., Li, W., Wei, Z., Peng, J., Yi, Y., and Wu, P. (2023). Methods and experiments for collecting information and constructing models of bottom-layer contours in paddy fields. *Computers and Electronics in Agriculture* **2023**, *207*, 107719, doi:10.1016/j.compag.2023.107719
21. Flintsch, G. W., Valeri, S. M., Katicha, S. W., de Leon Izeppi, E. D., and Medina-Flintsch, A. Probe vehicles used to measure road ride quality: Pilot demonstration. *Transportation research record* **2012**, *2304*, 158-165, doi:10.3141/2304-18
22. Liu, Y., Wang, G., Yang, Y., Liu, J., and Sun, L. Road surface equivalent reconstruction based on measured road spectrum. *Transactions of the Chinese Society of Agricultural Engineering* **2012**, *28*, 26-32, doi:10.3969/j.issn.1002-6819.2012.19.004
23. Choi, M., Kim, M., Kim, G., Kim, S., Park, S., and Lee, S. 3D scanning technique for obtaining road surface and its applications. *International Journal of Precision Engineering and Manufacturing* **2017**, *18*, 367-373, doi:10.1007/s12541-017-0044-1
24. Zhanfeng, H., Zhixiong, L., and Lanying, Z. Fractal behavior of tillage soil surface roughness. *Transactions of the Chinese Society of Agricultural Machinery* **2007**, *38*, 50-53.
25. Lu, Z., Zhao, L., and Hou, Z. Fractal behavior of road profile roughness. *Journal of Jiangsu University (Natural Science Edition)* **2008**, *29*, 111-114.
26. Wang, L., Yan, J., Hou, Z., and Zhang, Y. Design and experiment on agricultural field profiling apparatus. *Journal of Shenyang Agricultural University* **2018**, *49*, 425-432, doi:10.3969/j.issn.1000-1700.2018.04.006
27. Zhu, S., Ma, J., Yuan, J., Xu, G., Zhou, Y., and Deng, X. Vibration characteristics of tractor in condition of paddy operation. *Transactions of the Chinese Society of Agricultural Engineering* **2016**, *32*, 31-38, doi:10.11975/j.issn.1002-6819.2016.11.005
28. Zhao, R., Hu, L., Luo, X., Zhou, H., Du, P., Tang, L., He, J., and Mao, T. A novel approach for describing and classifying the unevenness of the bottom layer of paddy fields. *Computers and Electronics in Agriculture* **2019**, *162*, 552-560, doi:10.1016/j.compag.2019.05.001
29. Balduzzi, M. A., Van der Zande, D., Stuckens, J., Verstraeten, W. W., and Coppin, P. The properties of terrestrial laser system intensity for measuring leaf geometries: a case study with conference pear trees (Pyrus Communis). *Sensors* **2011**, *11*, 1657-1681, doi:10.3390/s110201657
30. Starek, M. J., Chu, T., Mitasova, H., and Harmon, R. S. Viewshed simulation and optimization for digital terrain modelling with terrestrial laser scanning. *International Journal of Remote Sensing* **2020**, *41*, 6409-6426, doi:10.1109/78.923297